Raman Spectroscopy and Dioxygen Adsorption on Cs-Loaded Zeolite Catalysts for Butene Isomerization

Junhui Li and Robert J. Davis*

Department of Chemical Engineering, University of Virginia, 102 Engineers Way, Charlottesville, Virginia 22904-4741

Received: October 27, 2004; In Final Form: January 19, 2005

Cesium-exchanged zeolite X was impregnated with cesium acetate (Cs(Ac)/CsX) or cesium carbonate (Cs_2CO_3/CsX) and subsequently calcined to yield a basic catalyst. The Raman spectra of calcined Cs(Ac)/CsX and Cs_2CO_3/CsX exhibited a new peak at 1036 cm^{-1} associated with the occluded species. No evidence for cesium peroxide or superoxide was observed. The occluded cesium species in both samples is proposed to be an oxycarbonate, which is a metastable intermediate between cesium carbonate and cesium oxide. The isomerization of 1-butene to *cis*- and *trans*-2-butene was catalyzed by cesium-loaded zeolite X. Although CO_2 readily poisoned the active base sites for catalysis, pretreatment of a basic zeolite with O_2 at 373 K did not. Co-feeding O_2 with 1-butene at 373 K, however, completely deactivated the base sites. Analysis of the reactor effluent at 473 K and the IR spectrum of the catalyst indicated the formation of carbon dioxide, which irreversibly adsorbed on the basic sites of the catalyst. Deactivation of basic catalysts by O_2 is proposed to occur through a low temperature oxidation of 1-butene to carbon dioxide, which strongly adsorbs on the active sites.

Introduction

Heterogeneous base catalysts have attracted significant attention in recent years because they are active and selective for many kinds of reactions, including isomerization, dehydrogenation, amination, hydrogenation, alkylation, and condensation.[1] Although numerous reactions are carried out industrially by liquid base catalysts, the replacement of liquid bases by solid base catalysts would have the advantage of decreasing corrosion and environmental problems, while allowing easier separation and recovery of the catalysts.[1−3] Commercialization of heterogeneous base catalysts is still in its infancy as compared with heterogeneous acid catalysts. Tanabe and Holderich performed a survey that indicated 103, 10, and 14 industrial processes use solid acids, solid bases, and acid−base bifunctional catalysts, respectively.[4] A high deactivation rate and a need for severe pretreatment conditions may be some of the reasons impeding the application of solid basic catalysts. Therefore, fundamental studies on the structure, reactivity, and deactivation of solid bases are needed before they can be used as widely as solid acids.

Alkali ion-exchanged zeolites X and Y are recognized to be weak bases. The origin of the basicity is the oxygen ions in the negatively charged zeolite framework.[1,5] The overall basic strength of alkali ion-exchanged zeolites has been ranked according to the negative charge of the oxygen atoms calculated by Sanderson's electronegativity equalization principle.[6] Thus, the basic strength of the X-zeolite is greater than that of the corresponding Y-zeolite because of the higher framework negative charge of the former. In addition, the basic strength depends on the nature of the exchangeable cations and increases in the order Li < Na < K < Rb < Cs.[7] This trend was confirmed experimentally by X-ray photoelectron spectroscopy (XPS) of the zeolites[8,9] and infrared spectroscopy of the adsorbed pyrrole.[10] One of the advantages of using weak bases in a process is ease of handling. Weak bases can be manipulated in ambient atmosphere, and thermal pretreatment will remove weakly adsorbed carbon dioxide and water. Weak bases can be also used in reactions in which water and CO_2 are reactants or products. However, the low basic strength of ion-exchanged zeolites is inadequate for a reaction such as olefin isomerization.

Generally, there are several ways to increase the zeolite basicity by postsynthetic modification. Martens et al. formed metallic sodium particles in zeolites by the decomposition of occluded sodium azide.[11] These sodium particles are capable of catalyzing reactions involving carbanion-like intermediates, such as the double bond isomerization of 1-butene at 300 K. Hathaway and Davis impregnated CsNaX and CsNaY with cesium acetate and thermally decomposed the occluded acetate in zeolite supported base catalysts.[12,13] Since then, many reactions have been performed on similarly prepared catalysts.[14−23] Li and Davis reported that the active site density for strong base catalysis on cesium-loaded zeolite X is very low, which makes the catalyst vulnerable to the trace impurities in the feed.[14] Zeolites loaded with ytterbium or europium also showed high activity for the double bond isomerization of 1-butene at 273 K.[24−28] The isomerization proceeds via allylic−carbanion type intermediates, indicating that zeolites act as basic catalysts.

Zeolites provide a solvent-like environment in which the framework atoms interact with the occluded clusters in the cages.[5] Experiments show that the cesium species within the pores of zeolites have different properties than cesium entrapped in other microporous materials.[16,19]

Several characterization methods have been devoted to the investigation of the alkali metal species occluded in zeolites, including various spectroscopic techniques such as infrared (IR), solid-state nuclear magnetic resonance (NMR), X-ray absorption, and XPS.[13−23,29,30] Gas adsorption studies, like N_2 adsorption, CO_2 adsorption microcalorimetry, and temperature-programmed desorption of various probe molecules, have been

* Corresponding author. E-mail: rjd4f@virginia.edu.

10.1021/jp045092j CCC: $30.25
Published on Web 03/18/2005

extensively performed.[14−23] Investigations by Hathaway and Davis showed that FT-IR bands associated with the occluded cesium acetate disappeared after being heated to 623 K for 30 min. Moreover, small broad bands were observed at 723 K between 1710 and 1366 cm^{-1}, which are in the region of adsorbed carbonate.[13] Kim et al. reported that the ^{133}Cs NMR spectra of cesium species occluded in zeolites are significantly different than bulk Cs_2O.[19] Although a significant level of understanding of alkali-loaded base catalysts has already been achieved, the state of the alkali metal species and the mechanism to form the strong basic sites in alkali metal-loaded zeolites are still not understood. In this work, Raman spectroscopy was utilized to characterize vibrational frequencies of the occluded species, and 1-butene isomerization in the presence of O_2 was used to probe the reactivity of the catalyst.

Experimental Procedures

Catalyst Preparation. Ion-exchanged CsX zeolite was prepared according to procedures described in ref 14. NaX (Union Carbide, lot 07483−36) was triply ion exchanged with 1 M aqueous solutions of cesium acetate (Aldrich 99.9%) at room temperature. The ion-exchanged samples were then washed with distilled deionized water (>1 L per g of zeolite). Zeolites containing excess alkali species (in addition to the ion-exchanged cations) were prepared by impregnation of the ion-exchanged zeolites with a cesium acetate (Aldrich, 99.99%) or cesium carbonate (Aldrich, 99.9%) solution. The concentrations of the cesium salts were determined by the desired Cs loading and by the amount of water the zeolite can absorb during the wet impregnation. The cesium-loaded zeolites were denoted as Cs(Ac)/CsX and Cs_2CO_3/CsX, indicating the cesium acetate and cesium carbonate precursors, respectively. The number listed in the parentheses after the name of the catalyst denotes the Cs loading of the catalyst, which has the units of excess cesium atoms/unit cell. The impregnated catalysts were dried overnight in air at 373 K and calcined in flowing air at 773 K for 5 h. Cs(Ac)/γ-Al_2O_3 was also prepared to explore the effect of zeolite structure on the excess cesium species. The γ-Al_2O_3 support was obtained from Mager Scientific Inc. Cs(Ac)/γ-Al_2O_3 was obtained by incipient wetness impregnation of the alumina support with aqueous solution of cesium acetate with an appropriate concentration.

X-ray Diffraction. Powder X-ray diffraction studies were conducted on a Scintag XDS 2000 diffractometer, using a CuKα source with a wavelength of 0.154060 nm. The X-ray patterns were collected with a scan rate of 1 deg min^{-1} and a step size of 0.03°.

Temperature Programmed Desorption (TPD) of Dioxygen and Stepwise TPD (STPD) of Carbon Dioxide. The TPD of O_2 (BOC Gases, 99.999%) was performed to explore the nature of occluded cesium species. To ensure the gas purity, helium (BOC Gases, 99.999%) and dioxygen were pretreated further by an OMI-2 indicating purifier (Supelco) and a moisture trap (Alltech, 400 mL), respectively. Approximately 800 mg of the sample was loaded into the ceramic pan. The temperature was ramped from 303 to 773 K at 4 K per min, followed by an isothermal step at 773 K for 300 min in helium. Next, the sample was cooled to 373 K and kept at 373 K for 105 min. For the first 15 min, only pure helium was allowed to flow. A mixture of dioxygen and helium was fed at 180 mL min^{-1} with 10% dioxygen for a 30 min period. The feed was switched back to pure helium to desorb any weakly adsorbed dioxygen from the surface and to purge the sample chamber. After purging, the temperature was ramped at 3 K per min to 773 K and kept isothermal for 120 min. The catalyst was characterized with STPD of CO_2 (BOC Gases, Spectra-Clean) to determine the number and strength of the basic sites on our catalysts. The details of STPD of CO_2 can be found in ref 14.

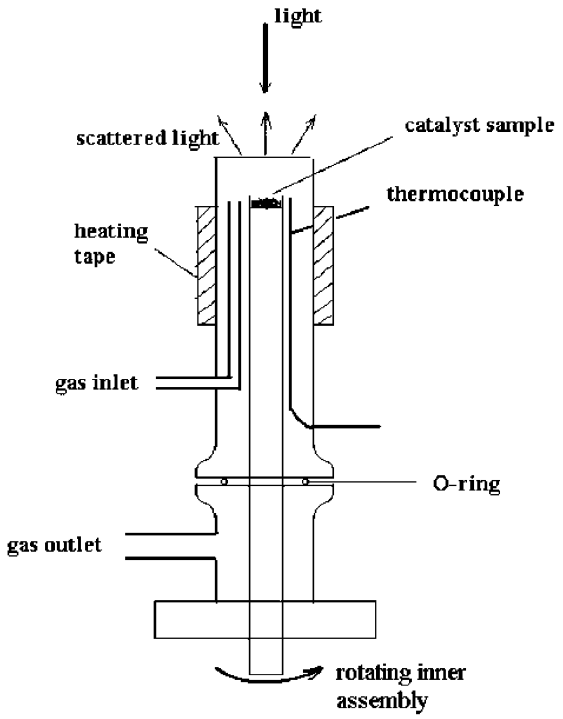

Figure 1. Schematic of in situ Raman cell.

In Situ Raman Spectroscopy of Base Catalysts. Raman spectra were collected with a Jobin Yvon-Spex TRIAX 550 with 600 grooves/mm grating, together with a Melles Griot He−Ne laser having an excitation line at 632.8 nm. The resolution of the Raman spectrometer is 2 cm^{-1}. A quartz, in situ cell used in the Raman experiment is depicted in Figure 1. Powder catalysts were placed in the sample holder located within a quartz cell. As the Raman spectrum was recorded, the sample holder was rotated to reduce laser heating.[31,32] The catalyst was heated at 773 K overnight in He/O_2 (3:1, BOC Gases, 99.999%) to reduce the fluorescence emission. After heating, the sample was cooled to 373 K for data collection unless otherwise noted. The spectrum reported here was an average of 1000 scans.

Sodium peroxide (97%), cesium carbonate (99.9%), and Cs_2O (which is actually a mixture of peroxide and superoxide) were purchased from Aldrich.

Analysis of Peroxide. Trace amounts of hydrogen peroxide can be detected by the titanium sulfate/spectrophotometric method.[33] This method is normally used for determining residual H_2O_2 present in water in concentrations ranging from 1 to 10 mg L^{-1}. The method involves reacting a sample containing H_2O_2 with titanium−sulfuric solution to produce a yellow peroxo-complex, which is then analyzed by a spectrophotometer at 405 nm.

Eisenberg described the preparation of a titanium−sulfuric solution.[33] Hydrogen peroxide solutions with different concentrations were also prepared for calibration purposes and were mixed with a 1 mL aliquot of the titanium−sulfuric solution.

For our zeolite materials, the possibility exists that cesium peroxide is located in the zeolite pores. However, it should react with water at room temperature to form hydrogen peroxide according to[34]

$$Cs_2O_2 + H_2O \leftrightarrow 2CsOH + H_2O_2$$

The titanium sulfate/spectrophotometric method can thus used to determine the presence of cesium peroxide. About 1 g of Cs(Ac)/CsX (14) was pretreated in an airtight vessel flowing with He (BOC Gases, 99.999%, 100 mL min^{-1}) at 773 K for 5 h.

Next, 5 mL of deionized water was added to the vessel. This slurry was filtered, and the solution was mixed with 1 mL of titanium sulfate solution. The color of the resulting solution was monitored by a spectrophotometer.

Catalytic Activity in 1-Butene Isomerization. Catalytic reactions were performed in a single-pass, fixed-bed, quartz-tube reactor. The catalysts were pretreated in situ at 773 K for 300 min under flowing helium (BOC Gases, 99.999%, 35 mL min^{-1}). The total flow rate of the feed stream, 16% 1-butene (Aldrich, 99+%) in helium, was approximately 25 mL min^{-1}. Before the feed stream was introduced into the reactor, 1-butene was purified with 3 Å molecular sieves to remove trace impurities. The reaction was always carried out at 373 K, unless otherwise noted. Reaction products were analyzed online by an HP5890 II gas chromatograph equipped with a flame ionization detector. A Chrompak 50 m, 0.32 mm ID alumina/KCl plot column with a film thickness of 0.10 μm was used for product separation.

Addition of O_2 to Reaction. A sample was first pretreated in situ at 773 K for 300 min under flowing helium (BOC Gases, 99.999%, 35 mL min^{-1}). Next, the catalyst was exposed to 35 mL min^{-1} He and 4 mL min^{-1} O_2 (BOC Gases, 99.999%) at 373 or 473 K for 10 min. Finally, catalysts were purged with He (35 mL min^{-1}) at 373 or 473 K for different periods of time, and 1-butene isomerization was performed at 373 or 473 K. Products from the reaction were analyzed online by an HP5890 II gas chromatograph equipped with a flame ionization detector (FID) and a thermal conductivity detector (TCD).

In Situ Infrared Spectroscopy of Cs-Loaded Catalysts. Cesium-loaded zeolite was pressed into a self-supporting pellet and loaded into a cell for IR spectroscopy. The sample was pretreated in flowing He (100 mL min^{-1}, 99.999%, BOC Gases, further purified with a Supelco OMI-2 purifier) at 773 K for 5 h before cooling. A Pfieffer turbomolecular pump was used to evacuate the cell to 9.6×10^{-5} Torr while cooling. Absorbance spectra of the catalyst were averaged from 300 scans at 473 K collected on a Bio Rad FTS-60A spectrometer operating with a resolution of 2 cm^{-1}. A mixture of O_2 (50 mL min^{-1}) and 1-butene (5 mL min^{-1}) was co-fed into the in situ infrared cell. The absorbance spectra were recorded at different times.

Results and Discussion

Composition of Zeolites and Characterization by X-ray Powder Diffraction. Elemental analysis of commercial NaX, ion-exchanged CsX, and Cs-loaded CsX has been performed extensively in the previous work of our lab.[15,16,35] The typical unit cell composition of commercial NaX from Union Carbide was $H_{8.9}Na_{78.8}Si_{104.3}Al_{87.7}O_{384}$, which indicated that the Si/Al ratio was 1.2. The compositions of CsX from six different batches were averaged to be $Na_{34.4}Cs_{44}Si_{104}Al_{87.7}O_{384}$, and the degree of exchange of Cs^+ with Na^+ was therefore about 56%. Bordawekar and Davis observed that the CO_2 adsorption capacity of Cs-loaded zeolite X and Y increased linearly with the amount of occluded cesium atoms.[16] The stoichiometry of adsorption was measured to be about one CO_2 adsorbed for every four occluded cesium atoms.[16] We have also confirmed the same linear relationship of CO_2 adsorbed with nominal loading of occluded Cs in zeolite X and the same adsorption stoichiometry.[14]

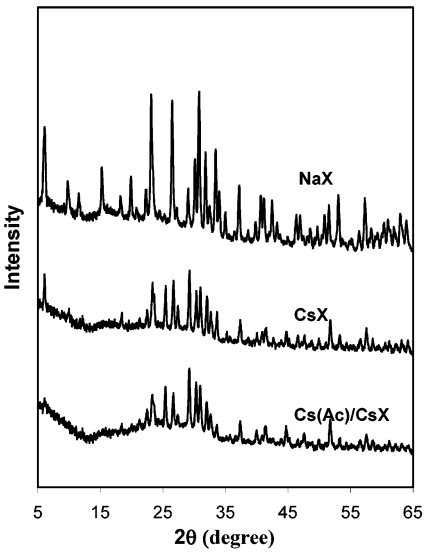

Figure 2. X-ray powder diffraction of NaX, CsX, and Cs(Ac)/CsX-(14).

TABLE 1: Dioxygen Adsorption Capacity of Cs-Containing Zeolite X

catalyst	O_2 uptake (μmol g^{-1})[a]	normalized O_2 adsorption capacity (μmol/μmol ex Cs)[b]
KX	5	
Cs(Ac)/KX (16)	12	6×10^{-3}
CsX	8	
Cs(Ac)/CsX (10)	13	7×10^{-3}

[a] The partial pressure of O_2 was 0.10 bar. [b] ex = excess.

The X-ray powder patterns of NaX, CsX, and Cs(Ac)/CsX (14) are presented in Figure 2. A decrease in the peak intensity for Cs-containing samples is due to the strong absorption of X-rays by Cs as compared to Na. No evidence for cesium salt crystallites on the external surface of the zeolite was observed. Earlier work indicates that the excess of the cesium species is located primarily in the zeolite supercages for the samples containing up to 24 cesium atoms per unit cell.[16,21] Since the number of occluded cesium atoms in our samples was always less than 24 Cs/unit cell, most of the cesium should be located in the zeolite supercages. The relatively high surface area and the high catalytic activity for 1-butene isomerization over the Cs(Ac)/CsX discussed in our previous paper are consistent with the excess cesium species being occluded in the supercage.[14]

Marra et al. characterized the cation distributions of RbNaY with low-temperature infrared spectroscopy and XRD.[36] They concluded that Rb^+ cations have substituted nearly all Na^+ ions of the site SII, which is located near or inside the supercage. The remaining Na^+ cations therefore must be located inside hexagonal prisms or sodalite cavities and therefore inaccessible to most of the molecules. It is assumed that CsNaX is similar to RbNaY with most of the Cs^+ cations located at the sites near or in the supercage, while the residual Na^+ ions would be located inside hexagonal prisms or sodalite cavities. For Cs(Ac)/CsX or Cs_2CO_3/CsX, the occluded clusters inside the supercage of the zeolites are far away from the remaining Na^+ but close to the exchangeable Cs^+ cations. Therefore, it is reasonable to neglect the effect of the remaining Na^+ on the occluded species.

TPD of O_2 and Stepwise TPD (STPD) of CO_2 on Basic Zeolites. Table 1 summarizes the results from TPD of O_2 on zeolite X. The values of O_2 uptake were very low and therefore contained substantial uncertainty, approximated to be 30%. About 8 and 5 μmol g^{-1} dioxygen adsorbed on CsX and KX,

respectively. Bajusz et al. studied the adsorption of N_2 and O_2 on CaX by an isotopic-transient method.[37] The authors found that around 27 μmol g^{-1} O_2 adsorbed on CaX at 303 K when exposed to a partial pressure of 0.13 bar. Both dinitrogen and dioxygen are capable of electrostatic interactions with the zeolite surface because they possess quadrupole moments. The Ca^{2+} ions in CaX have a higher charge density (32 C $m^{-3} \times 10^{-10}$) than the Cs^+ ions in CsX (9.6 C $m^{-3} \times 10^{-10}$), which accounts for the higher dioxygen adsorption capacity of CaX.[37]

According to the experimental results in Table 1, zeolites containing cesium in excess of the ion-exchanged capacity (Cs-(Ac)/CsX or Cs(Ac)/KX) adsorbed more dioxygen than the ion-exchanged zeolites (CsX or KX). The difference in dioxygen adsorption between cesium-loaded and ion-exchanged zeolites is considered to be the amount of O_2 adsorbed on the excess cesium species. Extra framework cations in zeolite X may be located in the double six-rings, β-cages, and supercages. However, due to steric factors, dioxygen cannot enter the β-cages and interacts with cations located only in the supercages.[38] The occluded cesium ions evidently contributed to the higher dioxygen adsorption capacity of cesium-loaded zeolites. However, the amount of dioxygen adsorbed was very small as compared to the amount of the excess cesium species occluded in zeolite X. For 1000 occluded cesium ions, only about six to seven dioxygen molecules were adsorbed on Cs(Ac)/KX (16) and Cs(Ac)/CsX (14).

Yagi and Hattori reported that the amount of dioxygen adsorbed on the cesium- loaded zeolite X (~9 wt % of cesium atoms) was 3.9 μmol g^{-1} with an equilibrium pressure of 7.8 kPa at 293 K on cesium-added CsX, which is somewhat lower than the values reported here.[22]

Jasra et al. reported that the heat of adsorption for dioxygen on cesium exchanged NaX was around 12 kJ mol^{-1}, indicating that dioxygen only weakly physisorbed on the ion-exchanged zeolite.[38] The microcalorimetric results of Bordawekar and Davis showed no chemisorption of dioxygen on cesium-loaded zeolite X, presumably because the heat of adsorption was below the detection limit of the microcalorimeter.[16]

The results from CO_2 STPD of various catalysts are presented in Figure 3. The total uptakes of CO_2 were about 202, 152, 239, and 269 μmol g^{-1} for Cs(Ac)/CsX (14), Cs_2CO_3/CsX (12), Cs_2CO_3/CsX (18), and Cs_2CO_3/CsX (23, He), respectively. The adsorption capacities correspond to a stoichiometry of one CO_2 adsorbed per four occluded Cs atoms, which is consistent with earlier work[14,16] and confirms a very high dispersion of the occluded cesium in our current samples. In a previous study, we demonstrated that about 80% of the activity of Cs(Ac)/CsX and Cs(Ac)/KX in 1-butene double-bond isomerization arose from the basic sites that desorbed CO_2 between 673 and 773 K.[14] The amounts of carbon dioxide desorbed between 673 and 773 K were 17, 13, 20, and 8 μmol for 1 g of Cs(Ac)/CsX (14), Cs_2CO_3/CsX (12), Cs_2CO_3/CsX (18), and Cs_2CO_3/CsX (23, He), respectively. However, most of the CO_2 desorbed below 573 K, as indicated in Figure 3.

In Situ Raman Spectroscopy. Infrared spectroscopy is an efficient characterization tool for many heterogeneous catalysts and has been used widely for the exploration of basic zeolites. However, some of the possible alkali metal species occluded in zeolites, such as oxide (O^{2-}), peroxide (O_2^{2-}), or superoxide (O_2^-) anions, exhibit weak infrared absorption features. For example, the peroxidic bond is symmetrical and hence does not induce great changes in the dipole moment, and the IR absorption could be weak or even absent.[39] As a complementary method to infrared spectroscopy, Raman spectroscopy is an efficient tool for directly probing organic, organometallic, or inorganic compounds entrapped in the pore system of zeolites.[40] Since zeolite catalysts are very sensitive to adsorbed molecules, information on the active sites can only be obtained after high-temperature pretreatment in a high purity carrier gas. Raman spectroscopy is a method particularly suitable for in situ studies at high temperatures.[31,32]

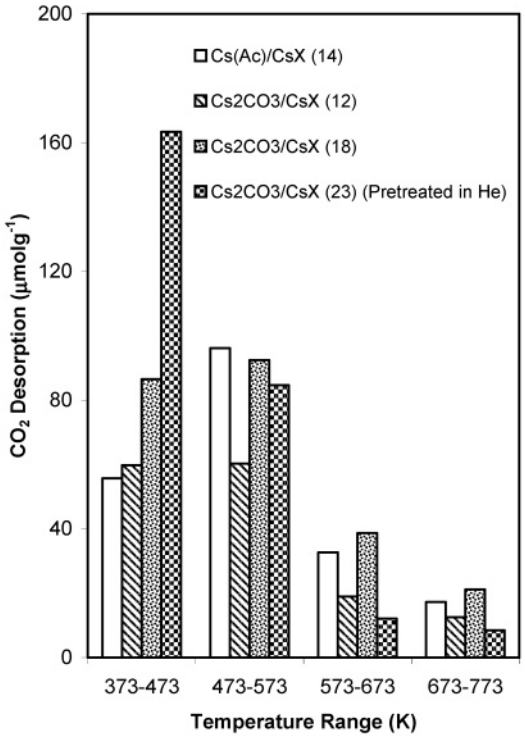

Figure 3. Stepwise TPD of CO_2 from different cesium-loaded zeolites.

Cesium oxide reacts with oxygen to form cesium peroxide or cesium superoxide in a highly exothermic reaction.[41,42] The standard molar enthalpy of Cs_2O oxidation has been reported to be about 449 ± 25 kJ mol^{-1} ($Cs_2O + 0.5O_2 = Cs_2O_2$).[41−43] In addition, experimental and density functional theory (DFT) calculation results showed that the adsorption heat of carbon dioxide ($-\Delta H_{ads}$) on Cs_2O is about 280 kJ mol^{-1}, which is much higher than the CO_2 adsorption heat on the cesium-loaded zeolite X (~100 kJ mol^{-1}).[14,16,44] At an oxygen pressure of 10^{-15} bar, Lamoreaux et al. revealed that Cs_2O_2 is the stable phase below 620 K and that Cs_2O is stable from this temperature to its melting point.[41] In a relatively high oxygen pressure (0.2 bar), CsO_2 is the most stable oxide.

The Raman spectra of dehydrated faujasite-type zeolites have been extensively studied. Ion-exchanged cesium zeolite X has a strong peak at 510 cm^{-1} that results from in-plane bending or deformation of O−T−O, in which T represents Si or Al. In our experiments, all zeolitic catalysts had a Raman band near 510 cm^{-1}, the value of which agrees well with published results.[45−49]

Figure 4 reports the characteristic Raman spectra of several standard samples collected at 373 K. The Raman shift of O_2^- in CsO_2 was 1134 cm^{-1} (Figure 4a) and for O_2^{2-} in Na_2O_2 was 738 and 792 cm^{-1} (Figure 4b). In Figure 4c, the feature at 1051 cm^{-1} is the C−O symmetric stretch of CO_3^{2-} in Cs_2CO_3. All the features associated with standard compounds are in good agreement with published spectra.[39,40,50,51] Although cesium carbonate decomposes at 883 K, it remained completely intact after calcination at 773 K (Figure 4c).

Figure 5 shows the Raman spectra of cesium-loaded zeolites. The sample Cs_2CO_3/CsX (23) in Figure 5a was exposed to

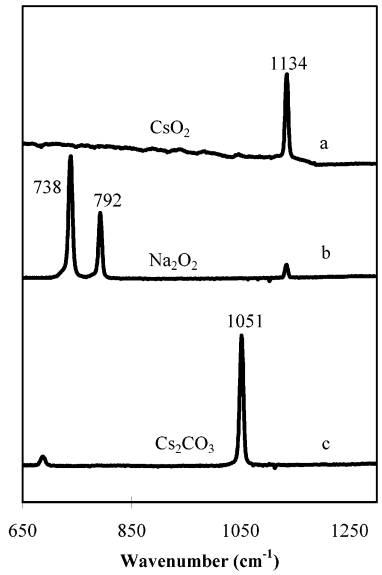

Figure 4. Raman spectra of (a) CsO_2; (b) Na_2O_2; and (c) Cs_2CO_3 (pretreated in He/O_2 at 773 K for 5 h) at 373 K.

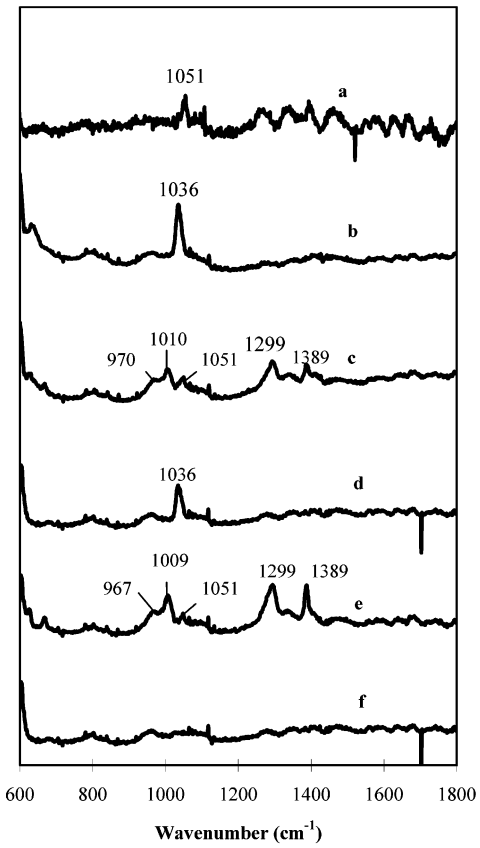

Figure 5. Raman spectra of cesium-loaded zeolites (a) Cs_2CO_3/CsX (23), before pretreatment, exposed to ambient air at room temperature; (b) Cs_2CO_3/CsX (23), after pretreatment in He/O_2 at 773 K for 5 h after (a); (c) Cs_2CO_3/CsX (23), introduced CO_2 after (b); (d) Cs(Ac)/CsX (16), after pretreatment in He/O_2 at 773 K for 5 h; (e) Cs(Ac)/CsX (16), introduced in CO_2 after (d); and (f) CsX, after pretreatment in He/O_2 at 773 K for 5 h.

ambient air at room temperature before pretreatment. A characteristic peak at 1051 cm^{-1} indicated the presence of cesium carbonate. The poor signal/noise ratio of Figure 5a might be due to the fluorescence caused by impurities on the catalyst before calcination. Figure 5b,d,f shows Cs_2CO_3/CsX (23), Cs(Ac)/CsX (16), and CsX, respectively, after being pretreated at

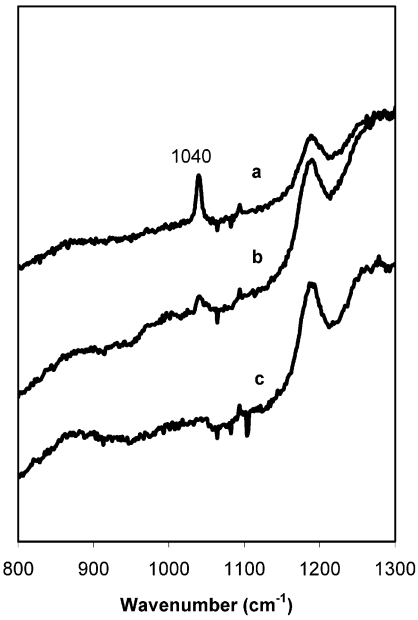

Figure 6. Raman spectra of (a) Cs(Ac)/γ-alumina (23.6 wt %), pretreated in He/O_2 at 773 K for 5 h; (b) introduced in CO_2 after (a); (c) γ-alumina, pretreated in He/O_2 at 773 K for 5 h.

773 K in He/O_2 (3:1) for 5 h. No Raman feature associated with cesium peroxide was observed. Figure 5b,d revealed the presence of a new peak at 1036 cm^{-1} and the disappearance of the peak at 1051 cm^{-1} after pretreatment, which suggests that the impregnated cesium carbonate partially decomposed upon heating. Nevertheless, the peak at 1036 cm^{-1} is considered to arise from a carbonate structure because it is near the bulk carbonate peak. A peak located at 1036 cm^{-1} was also observed on Cs(Ac)/CsX (16) (Figure 5d). Since the feature at 1036 cm^{-1} was not observed on the Cs-exchanged zeolite X in Figure 5f, it must be associated with the cesium species occluded in the pores beyond ion-exchange capacity. The similarity of the Raman spectra of Cs(Ac)/CsX and Cs_2CO_3/CsX suggests that the occluded species was the same, regardless of the acetate or carbonate precursor used in the synthesis.

To further investigate the properties of the cesium species, CO_2 was introduced after pretreatment in He/O_2. Figure 5c,e shows the Raman spectra of Cs_2CO_3/CsX (23) and Cs(Ac)/CsX (16) after the introduction of carbon dioxide. The peak at 1036 cm^{-1} disappeared after CO_2 adsorption, and three small new bands at 970 (shoulder), 1010, and 1051 cm^{-1} were created. The assignment of these three bands is not clear. These peaks probably arise from symmetric C−O stretching of the carbonate structure of the occluded cesium species.

Three vibrations for free CO_2 are located at 1337 (ν_1), 667 (ν_2), and 2349 cm^{-1} (ν_3).[40] Thus, the Raman peaks at 1299 and 1389 cm^{-1} shown in Figure 5c,e after CO_2 adsorption were assigned to the $2\nu_2$ and ν_1 modes of carbon dioxide. In the gas phase, the $2\nu_2$ and ν_1 bands form a Fermi doublet at 1285 and 1388 cm^{-1}.[52] The ν_2 modes in Raman spectrum are forbidden by symmetry under the $D_{\infty h}$ point group. In our experiment, the activity of a forbidden mode ($2\nu_2$) is indicative of symmetry reduction due to CO_2 adsorption on the zeolite base catalysts. In addition, the $2\nu_2$ was blue-shifted by 14 cm^{-1} because of the interaction of carbon dioxide with the catalysts. The ν_1 mode disappeared after purging with He at 373 K and is attributed to weakly adsorbed CO_2.

The Raman spectra of Cs(Ac)/γ-Al_2O_3 (23 wt %) are summarized in Figure 6. The peak at 1040 cm^{-1} (Figure 6a),

TABLE 2: Isomerization of 1-Butene to *Cis*- and *Trans*-2-Butene at 373 K[a]

catalyst	Cs loading (Cs #/unit cell)	initial TOF (s^{-1})[b]	reaction rate (10^{-6} mol g^{-1} min^{-1})	cis/trans	conversion of 1-butene (%)
Cs_2CO_3	0		0		0.0
Cs^2CO_3/CsX (23, He)[c]	23	0.00694	520	6	48.7
Cs(Ac)/CsX (14)	14	0.0252	1149	6	61.0
Cs_2CO_3/CsX (12)	12	0.0211	825	6	44.1
Cs(Ac)/γ-Al_2O_3	23.6 (wt %)	0.00706	671	5	40.6

[a] Atmospheric pressure, $T = 373$ K; 16 mol % 1-butene in He; pretreated in air at 773 K. [b] The initial turnover frequency (TOF) was based on the number of product molecules formed during a short time on the stream (20 min) normalized by the amount of excess Cs occluded in the supercage of CsX or loaded on the surface of γ-Al_2O_3. [c] The catalyst was pretreated in helium at 773 K.

which is similar to the peak at 1036 cm^{-1} on Cs(Ac)/CsX and Cs_2CO_3/CsX, suggests that the calcination procedure might result in a similar cesium species, even with different supports (CsX and γ-alumina). However, the 4 cm^{-1} difference between the positions of the excess cesium species on CsX and on γ-alumina indicates some modification of the cesium species. The peak at 1040 cm^{-1} disappeared upon introduction of CO_2 at 373 K, which is illustrated in Figure 6b, indicating that the excess cesium species on γ-Al_2O_3 adsorbed CO_2. However, the forbidden mode of CO_2, $2\nu_2$, was not observed on Cs(Ac)/γ-Al_2O_3, indicating that there is little interaction between CO_2 and γ-Al_2O_3. The ν_1 mode of carbon dioxide was obscured by a peak corresponding to γ-alumina.

According to our experimental results, the occluded cesium species in zeolite X has a carbonate-like structure and interacts strongly with CO_2. Bordawekar et al. showed that the bulk cesium carbonate did not adsorb any CO_2 at 373 K even after being pretreated in a vacuum at 773 K.[16] Therefore, cesium carbonate was excluded as a possible candidate for the active sites of Cs-loaded zeolites and Cs-loaded alumina. Instead, we speculate that the species is an oxycarbonate. Stoichiometric cesium oxide is known to be extremely reactive.[49−51] Cesium oxide readily combines with carbon to form an oxycarbonate structure because of the poor stability of the cesium oxide. Apparently, this oxycarbonate is also more stable than cesium oxide in the zeolite pores. The carbon may originate from a trace amount of carbon dioxide in the air or the carbon atoms in cesium acetate or cesium carbonate precursors. Al-Shemali and Boldyrev studied the properties of Na_4CO_4 with ab initio methods.[53] They postulated various configurations having the Na_4CO_4 stoichiometry to test the stability of the orthocarbonate structure and found that that the orthocarbonate is a true minimum on the potential energy surface, but the most stable form is actually a complex of sodium carbonate and sodium oxide. The symmetric stretching frequency of C−O in sodium orthocarbonate is about 1036 or 1051 cm^{-1} according to two different calculation methods.[53] It is red-shifted by about 30−40 cm^{-1} as compared to the symmetric C−O stretching frequency of sodium carbonate (1080 cm^{-1}).[54] In our Raman experiments, the band position of occluded cesium species was red-shifted by 15 cm^{-1} as compared to bulk cesium carbonate. An isolated CO_4^{4-} anion is certainly unstable because of the high extra charge on the rather small penta-atomic CO_4 group, but countercations (Cs^+) can stabilize the tetravalent anion in the orthocarbonate structure.

Shirsat et al. found out that the lanthanum dioxycarbonate, $La_2O_2CO_3$, is a stable intermediate in the thermal decomposition of lanthanum carbonate. The lanthanum dioxycarbonate further decomposes to lanthanum oxide at higher temperatures (>993 K).[55] The lanthanum dioxycarbonate can be converted to monooxycarbonate, $La_2O(CO_3)_2$, by adsorption of carbon dioxide.[55] Other forms of oxycarbonate were also found with different metals, like barium, copper, and titanium.[56−57]

We also checked for the presence of trace amounts of cesium peroxide that might have been undetected by Raman spectroscopy. The titanium−sulfuric spectrophotometric analysis failed to reveal any traces of peroxide in Cs(Ac)/CsX (14), which is consistent with the lack of peroxide detected by Raman spectroscopy.

Catalytic Activity in 1-Butene Isomerization. Table 2 summarizes the activity of different base catalysts in 1-butene isomerization at 373 K. Bulk cesium carbonate showed no activity in the reaction, even after thermal activation at 773 K. The reaction rate of Cs(Ac)/CsX (14), Cs_2CO_3/CsX (12), and Cs_2CO_3/CsX (23, He) is in the ratio of 1.9:1.6:1. The amount of CO_2 desorbed between 673 and 773 K for those catalysts was in the ratio of 2.1:1.6:1 (Figure 3). This confirmed our previously reported observation that the activity of 1-butene isomerization on basic zeolites correlates to the amount of CO_2 desorbed above 673 K.[14]

The initial turnover frequency (TOF) was based on the number of product molecules formed at short time on-stream and normalized by the amount of excess cesium in the zeolite supercage. According to Table 2, Cs(Ac)/CsX (14) and Cs_2CO_3/CsX (12) had a similar TOF after pretreatment under the same conditions. In addition, the low activity of Cs_2CO_3/CsX (23, He), pretreated in helium at 773 K, indicates that either pretreatment with dioxygen is more effective for the production of active sites or that steric crowding lowers the observed activity of the high-loaded sample. The Cs(Ac)/γ-Al_2O_3 (23 wt %) sample exhibited lower 1-butene isomerization activity than Cs(Ac)/CsX (14). We speculate that the zeolite framework is more effective than alumina at stabilizing the strong base sites needed for the isomerization reaction.

Effect of Dioxygen on Catalytic Activity. When a pretreated fresh catalyst was exposed to O_2 and subsequently purged with He at 373 K after the introduction of O_2, the catalyst revealed a high activity. Figure 7 shows how the He purge time affects the recovery of the catalyst after O_2 exposure. The longer the time of the He purge, the higher the percentage of original activity is observed. Thus, for base catalysis, oxygen alone does not irreversibly poison the cesium-loaded zeolite X. Figure 8 shows the conversion of 1-butene in the isomerization reaction as a function of time and O_2 treatment over cesium-loaded zeolites.

Figure 9 illustrates the irreversible nature of the deactivation process. The addition of O_2 to a functioning zeolite catalyst halted the isomerization. The activity of the catalyst did not recover after cessation of the O_2 flow.

Trace amounts of carbon dioxide were detected by gas chromatography when 1-butene was co-fed with dioxygen at 373 K, indicating that 1-butene was completely oxidized on the basic zeolite at low temperature. The infrared spectra of Cs-(Ac)/CsX (14) obtained during the co-feed of O_2 and 1-butene at 473 K can be seen in Figure 10. The characteristic peak at 2339 cm^{-1}, indicating gas-phase CO_2, was observed on the

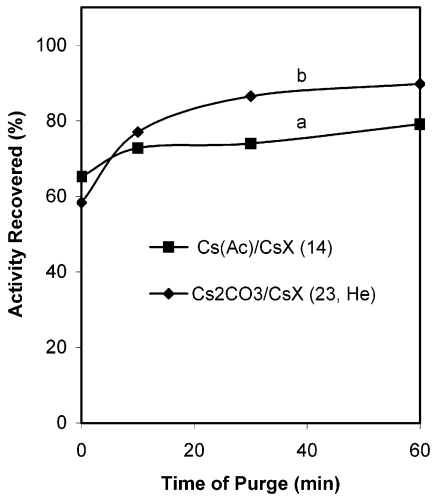

Figure 7. Influence of He purge time after O_2 exposure on recovery of 1-butene isomerization rate over two different Cs-loaded zeolites: (a) Cs(Ac)/CsX (14) and (b) Cs_2CO_3/CsX (23, He).

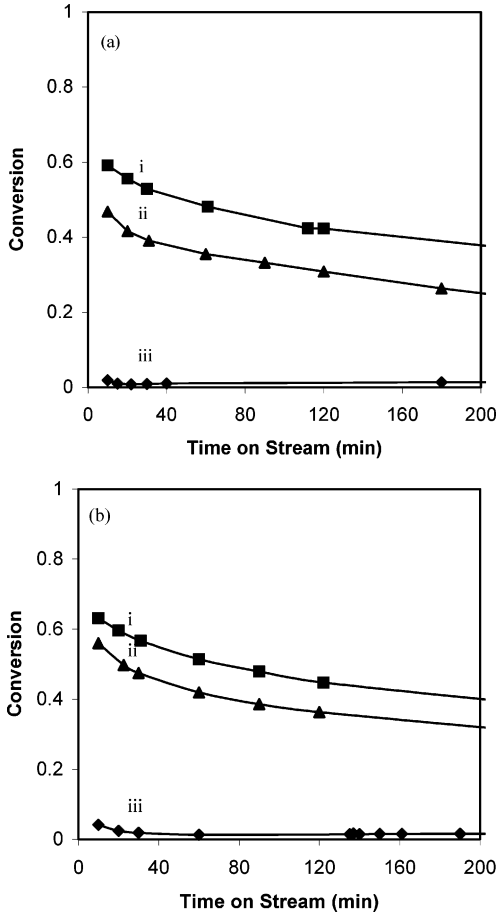

Figure 8. Reaction profiles for different conditions over basic zeolites (a) Cs(Ac)/CsX (14) and (b) Cs_2CO_3/CsX (23, He). (i) Standard 1-butene isomerization conditions; (ii) O_2 exposure, purged with He for 60 min; (iii) co-fed O_2 and 1-butene.

cesium-loaded zeolite as a product of complete oxidation of 1-butene. Another peak at 2361 cm^{-1} was due to a weak interaction between CO_2 and cesium cations and was attributed to the anti-symmetric stretching mode (ν_3) of the CO_2 molecule.[58] However, when O_2 or 1-butene was introduced alone into the system at 473 K, no carbon dioxide was observed in the system. Since our previous work showed that the cesium-loaded zeolites were totally poisoned by CO_2 adsorption at 373

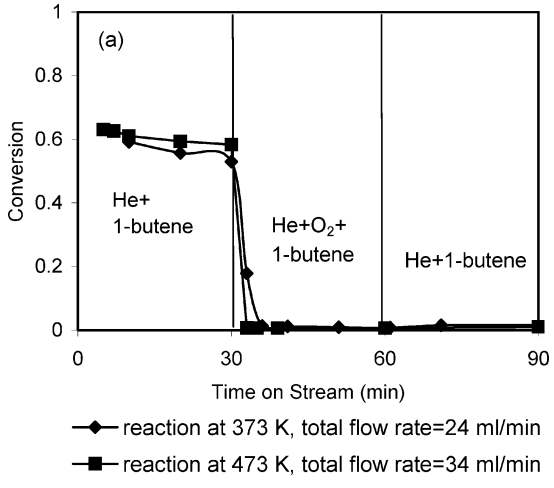

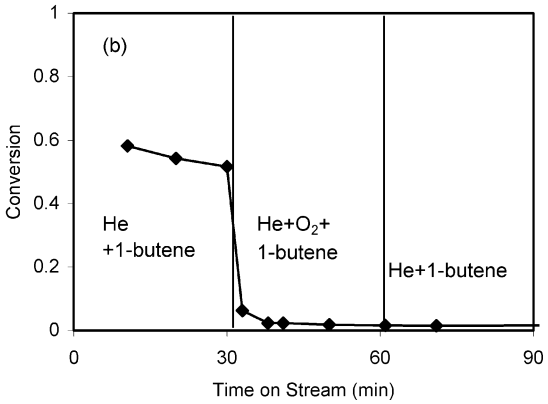

Figure 9. Irreversibility of O_2 deactivation of 1-butene isomerization over (a) Cs(Ac)/CsX (14) and (b) Cs_2CO_3/CsX (23, He).

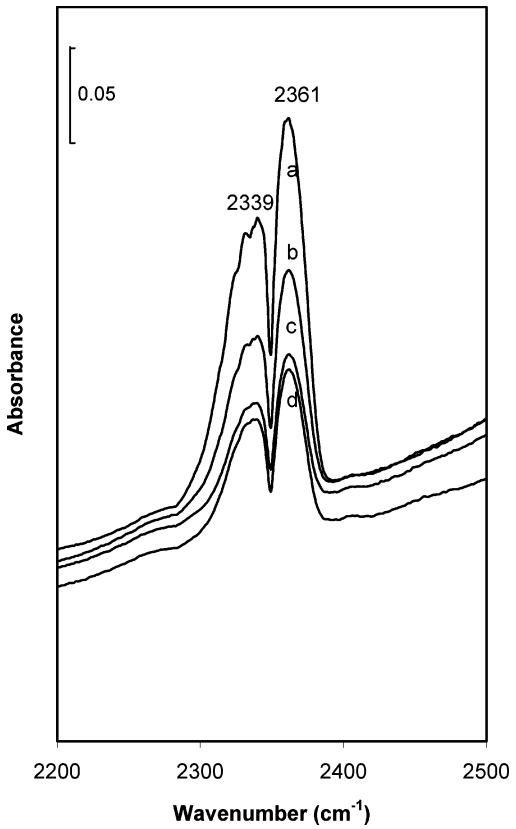

Figure 10. FT-IR spectra of Cs(Ac)/CsX (14) at 473 K in the presence of O_2 and 1-butene after (a) 5 min; (b) 10 min; (c) 20 min; and (d) 30 min.

K,[14] the deactivation of base-catalyzed butene isomerization by O_2 and 1-butene is likely due to CO_2 adsorption on the active sites. At 473 K, the amount of carbon dioxide detected in the gas phase was much larger than that at 373 K. Tang et al. used FT-IR spectroscopy to observe both photooxidation and thermal oxidation of 1-butene at ambient temperature over cationic forms of zeolite Y.[59] However, the mechanism of the dark thermal oxidation is still not clear. Further studies into this reaction are currently underway.

Conclusion

The similarity of the Raman spectra and catalytic activity of Cs_2CO_3/CsX and Cs(Ac)/CsX suggests that the nature of the occluded species was independent of the acetate or carbonate precursor used in synthesis. No evidence for peroxide was found in the activated, cesium-loaded zeolites. A Raman peak at 1036 cm^{-1} was associated with the occluded cesium species, which likely arises from some form of carbonate structure. Oxycarbonate is a metastable intermediate between cesium carbonate and cesium oxide that is a possible form of the cesium species occluded in CsX.

Pretreatment of the catalyst with dioxygen at 373 K did not deactivate the catalyst for butene isomerization, as long as it was purged with He. However, dioxygen poisoned the catalyst when it was co-fed with 1-butene. Since carbon dioxide was detected in the effluent from a reactor with co-fed dioxygen, the poisoning of the base-catalyzed butene isomerization resulted from a strong adsorption of CO_2 formed by low temperature butene oxidation.

Acknowledgment. This work was supported by the Department of Energy−Basic Energy Sciences (DEFG02-95ER14549).

References and Notes

(1) Hattori, H. *Chem. Rev.* **1995**, *95*, 537.
(2) Ono, Y.; Baba, T. *Catal. Today.* **1997**, *38*, 321.
(3) Davis, R. J. *J. Catal.* **2003**, *216*, 396.
(4) Tanabe, K.; Hölderich, W. F. *Appl. Catal., A* **1999**, *181*, 399.
(5) Barthomeuf, D. *Catal. Rev.-Sci. Eng.* **1996**, *38*, 521.
(6) Sanderson, R. *Chemical Bonds and Bond Energy*; Academic Press: New York, 1976.
(7) Mortier, W. J. *J. Catal.* **1978**, *56*, 138.
(8) Barr, T. L. *Zeolites* 1990, *10*, 760.
(9) Huang, M.; Agnot, A.; Kaliaguine, S. *J. Catal.* **1992**, *137*, 322.
(10) Huang, B.; Kaliaguine, S. *J. Chem. Soc., Faraday Trans.* **1992**, *88*, 751.
(11) Martens, L. R.; Grobet, P. J.; Jacobs, P. A. *Nature* **1985**, *315*, 568.
(12) Hathaway, P. E.; Davis, M. E. *J. Catal.* **1989**, *116*, 263.
(13) Hathaway, P. E.; Davis, M. E. *J. Catal.* **1989**, *116*, 279.
(14) Li, J.; Davis, R. J. *Appl. Catal., A* **2003**, *239*, 59.
(15) Doskocil, E. J.; Bordawekar, S. V.; Kaye, B. G.; Davis, R. J. *J. Phys. Chem. B* **1999**, *103*, 6277.
(16) Bordawekar, S. V.; Davis, R. J. *J. Catal.* **2000**, *189*, 79.
(17) Lasperas, M.; Cambon, H.; Brunel, D.; Rodriguez, I.; Geneste, P. *Microporous Mater.* **1993**, *1*, 343.
(18) Rodriguez, I.; Cambon, H.; Brunel, D.; Lasperas, M.; Geneste, P. *Stud. Surf. Sci. Catal.* **1993**, *78*, 623.
(19) Kim, J. C.; Li, H. X.; Chen, C. Y.; Davis, M. E. *Microporous Mater.* **1994**, *2*, 413.
(20) Tsuji, H.; Yagi, F.; Hattori, H. *Chem. Lett.* **1991**, 1881.
(21) Yagi, F.; Kanuka, N.; Tsuji, H.; Nakata, S.; Kita, H.; Hattori, H. *Microporous Mater.* **1997**, *9*, 229.
(22) Yagi F.; Tsuji, H.; Hattori, H. *Microporous Mater.* **1997**, *9*, 237.
(23) Yagi, F.; Hattori, H. *Microporous Mater.* **1997**, *9*, 247.
(24) Baba, T.; Koide, R.; Ono, Y. *J. Chem. Soc., Chem. Commun.* **1991**, 691.
(25) Baba, T.; Kim, G. J.; Ono, Y. *J. Chem. Soc., Faraday Trans.* **1992**, *88*, 891.
(26) Baba, T.; Hikita S.; Koide, R.; Ono, Y. *J. Chem. Soc., Faraday Trans.* **1993**, *89*, 3177.
(27) Baba, T.; Hikita, S.; Ono, Y.; Yoshida, T.; Tanaka, T.; Yoshida S. *J. Mol. Catal. A* **1995**, *98*, 81.
(28) Tanaka, T.; Yoshida, T.; Yoshida, S.; Baba, T.; Ono, Y. *Phys. B* **1995**, *208/209*, 687.
(29) Hunger, M.; Schenk, U.; Seiler, M.; Weitkamp J. *Angrew. Chem. Int. Ed. Engl.* **1997**, *36*, 2504.
(30) Hunger, M.; Schenk, U.; Seiler, M.; Weitkamp J. *J. Mol. Catal. A* **2000**, *156*, 153.
(31) Xie, S.; Iglesia, E.; Bell, A. T. *J. Phys. Chem. B* **2001**, *105*, 5144.
(32) Xie, S.; Rosynek, M. P.; Lunsford, J. H. *Appl. Spectrosc.* **1999**, *10*, 1183.
(33) Eisenberg, G. M. *Ind. Eng. Chem., Anal. Ed.* **1943**, *15*, 327.
(34) Greenwood, N. N.; Earnshaw, A. *Chemistry of the Elements*; Pergamon Press Inc.: New York, 1986.
(35) Tu, M.; Davis, R. J. *J. Catal.* **2001**, *199*, 85.
(36) Marra, G. L.; Fitch, A. N.; Zecchina, A.; Ricchiardi, G.; Salvalgaggio, M.; Bordiga, S.; Lamberti, C. *J. Phys. Chem. B* **1997**, *101*, 10653.
(37) Bajusz, I. G.; Goodwin, J. G. *Langmuir* **1998**, *14*, 2876.
(38) Jasra, R. V.; Choudary, N. V.; Bhat, S. G. T. *Ind. Eng. Chem. Res.* **1996**, *35*, 4221.
(39) Vacque, V.; Sombret, B.; Huvenne, P.; Legrand, S. S. *Spectrochim. Acta, Part A* **1997**, *53*, 55.
(40) Nakamoto, K. *Infrared and Raman Spectra of Inorganic and Coordination Compounds Part B: Application in Coordination, Organometallic, and Bioinorganic Chemistry*, 5th ed.; John Wiley & Sons: New York, 1997.
(41) Lamoreaux, R. H.; Hildenbrand, D. L. *J. Phys. Chem. Ref. Data.* **1984**, *13*, 151.
(42) Vannerberg, N.-G. *Prog. Inorg. Chem.* **1962**, *4*, 125.
(43) Krawietz, T. R.; Murray, D. K.; Haw, J. F. *J. Phys. Chem. A* **1998**, *102*, 8779.
(44) Tai, J.; Ge, Q.; Neurock, M.; Davis, R. J. *J. Phys. Chem. B* **2004**, *108*, 16798.
(45) Bremard, C.; Maire, M. L. *J. Phys. Chem.* **1993**, *97*, 9695.
(46) Huang, Y.; Leech, J. H.; Havenga, E. A.; Poissant, R. R. *Microporous Mesoporous Mater.* **2001**, *48*, 95.
(47) Knops-Gerrits, P. P.; De Vos, D. E.; Feijen, E. J. P.; Jacobs, P. A. *Microporous Mater.* **1997**, *8*, 3.
(48) Yu, Y.; Xiong, G.; Li, C.; Xiao, F. *Microporous Mesoporous Mater.* **2001**, *46*, 23.
(49) Dutta, P. K.; Zaykoski, R. E. *Zeolites* **1988**, *8*, 179.
(50) Hunter-Saphir, S. A.; Creighton, J. A. J. *Raman Spectrosc.* **1998**, *29*, 417.
(51) Wen, N.; Brooker, M. H. *J. Phys. Chem.* **1995**, *99*, 359.
(52) Maynard, K. J.; Moskovits, M. *J. Chem. Phys.* **1989**, *90*, 6668.
(53) Al-Shemali, M.; Boldyrev, A. I. *J. Phys. Chem. A* **2002**, *106*, 8951.
(54) Meekes, H.; Rasing, Th.; Wyder, P.; Janner, A.; Janssen, T. *Phys. Rev. B* **1986**, *34*, 4240.
(55) Shirsat, A. N, Ali, M.; Kaimal, K. N. G.; Bharradwaj, S. R.; Das, D. *Thermochim. Acta* **2003**, *399*, 167.
(56) Vasenkov, S.; Frei, H. *J. Phys. Chem. B* **1998**, *102*, 8177.
(57) Yashima, T.; Sato, K.; Hayasaka, T.; Hara, N. *J. Catal.* **1972**, *26*, 303.
(58) Lavalley, J. C. *Catal. Today* **1996**, *27*, 377.
(59) Tang, S. L. Y.; McGarvey, D. J.; Zholobenko, V. L. *Phys. Chem. Chem. Phys.* **2003**, *5*, 2699.